

Microwave response of a chiral Majorana interferometer

Dmitriy S. Shapiro^{1,2,3,*}, Alexander D. Mirlin^{4,5,6,7}, and Alexander Shnirman^{4,5}

¹*Dukhov Research Institute of Automatics (VNIIA), Moscow 127055, Russia*

²*Department of Physics, National Research University Higher School of Economics, Moscow 101000, Russia*

³*V. A. Kotel'nikov Institute of Radio Engineering and Electronics,
Russian Academy of Sciences, Moscow 125009, Russia*

⁴*Institut für Theorie der Kondensierten Materie,
Karlsruhe Institute of Technology, 76128 Karlsruhe, Germany*

⁵*Institute for Quantum Materials and Technologies (IQMT),
Karlsruhe Institute of Technology, 76021 Karlsruhe, Germany*

⁶*Petersburg Nuclear Physics Institute, St.Petersburg 188300, Russia and*

⁷*L. D. Landau Institute for Theoretical Physics, Semanova 1-a, 142432 Chernogolovka, Russia*

We consider an interferometer based on artificially induced topological superconductivity and chiral 1D Majorana fermions. The (non-topological) superconducting island inducing the superconducting correlations in the topological substrate is assumed to be floating. This allows probing the physics of interfering Majorana modes via microwave response, i.e., the frequency dependent impedance between the island and the earth. Namely, charging and discharging of the island is controlled by the time-delayed interference of chiral Majorana excitations in both normal and Andreev channels. We argue that microwave measurements provide a direct way to observe the physics of 1D chiral Majorana modes.

Introduction. Physics of artificial topological superconductors with chiral Majorana edge modes was a subject of intensive research during the last decade [1–4]. Initially, these systems were proposed in hybrid structures on surfaces of topological insulators, covered by regular superconductors and magnetic insulators [5]. Later on, heterostructures based on quantum anomalous Hall insulators (QAHI) combined with regular superconductors [6, 7] were experimentally studied. However, the reported evidence of the chiral Majorana fermions as half-quantized plateau in the two-terminal conductance [6] is under debate [8]. Further experimental advances were made in magnetic domains covered by superconducting monolayers [9] and in similar in spirit van der Waals heterostructures [10] (see also a theoretical proposal [11]). Surfaces of iron-based superconductors [12] showed signs of topological superconductivity. Alternative realization of 1D Majorana edges in magnetic materials showing a spin liquid phase was reported in [13].

Interferometers based on chiral Majorana modes should allow probing the nontrivial physics of these systems [14–24]. The first proposals addressed the dc-transport [14, 15]. Later, in a series of works the noise, braiding of Majorana edge vortices, and time resolved transport were studied [25–29].

Usually the regular superconductor, which induces the superconducting correlations in the topological material, is considered to have a fixed electrochemical potential. We, in contrast, consider a floating island. This allows us investigating the time resolved charging and discharging dynamics of the island, which can be measured using microwave experimental techniques.

Qualitative picture. We consider a system depicted symbolically in Fig. 1(a). Here, a single Ohmic contact serves as a source and a drain of chiral Dirac modes. As

the chiral Dirac mode approaches the superconducting area it is split into two chiral Majorana modes. The latter recombine later again into a chiral Dirac mode. We assume the lengths of the two Majorana branches, l_1 and l_2 , to be different, thus two different propagation times, $\tau_1 = l_1/v$ and $\tau_2 = l_2/v$. These time intervals determine the Thouless energy, $E_{\text{Th}} \equiv \frac{\hbar v}{\tau_1 + \tau_2}$, and another energy, $\Lambda \equiv \frac{\hbar v}{|\tau_1 - \tau_2|} \geq E_{\text{Th}}$. The superconducting island is floating and is characterized by a self-capacitance C_0 or, equivalently, by the charging energy $E_c = \frac{e^2}{2C_0}$.

Below, using the effective action technique we derive the admittance Y_ω (inverse impedance) of the island relative to the ground (source and drain), which is due to the currents in the edge modes. That is, Y_ω corresponds to the admittance between points 1 and 2 in Fig. 1 (a) without the self-capacitance C_0 . The total admittance between points 1 and 2 in Fig. 1(a) is a sum of Y_ω and that due to C_0 , i.e., $Y_\omega - i\omega C_0$. We obtain

$$Y_\omega/G_0 = 1 + \frac{(-1)^n \pi T}{\sinh \left[\pi T \frac{(l_2 - l_1)}{\hbar v} \right]} \frac{e^{i\frac{l_1}{v}\omega} - e^{i\frac{l_2}{v}\omega}}{i\omega}, \quad (1)$$

where $G_0 = e^2/(2\pi\hbar)$ is the conductance quantum.

To understand the physical meaning of the admittance Y_ω it is useful to plot the response $I(t)$ of the current flowing into the island to a voltage pulse $V(t)$ applied to the contact 1 of Fig. 1(a). This is, of course, given by $I(t) = \int dt_1 Y(t - t_1) V(t_1)$, where $Y(t)$ is the Fourier image of Y_ω . The responses to a delta-like and a step-like pulses at $T = 0$ are depicted in Figs. 2(a) and 2(b), respectively. The instantaneous response provided by the first term in Eq. (1) is explained by the immediate adjustment of the current in the outgoing Dirac mode to the new electrochemical potential of the island. This re-

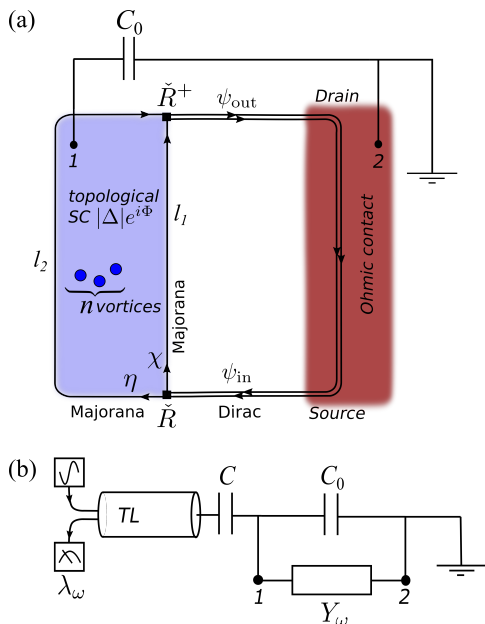


FIG. 1: (a) Schematic description of the Majorana interferometer with a floating superconducting island. Charge fluctuations on the island are allowed due to the finite self-capacitance $C_0 \neq \infty$. Incident Dirac mode ψ_{in} (doubled line) with equilibrium distribution function, imposed by the Ohmic contact, is scattered into a pair of Majorana modes (χ and η , single lines). χ and η coherently propagate along the edges of lengths l_1 and l_2 and are fused back into ψ_{out} . Scattering matrices of the lower and upper Y-splittings (black bars) are denoted by \tilde{R} and \tilde{R}^+ . Vortices in the superconductor induce an additional phase difference $n\pi$ between the interfering Majorana modes. (b) Equivalent electric circuit describing the interferometer in the linear response regime with a transmission line attached for measuring the microwave response. Points 1 and 2 correspond to to points 1 and 2 in the subfigure (a)). The input signal of a frequency ω is sent to a transmission line (TL) and a complex reflection coefficient λ_ω is measured. TL is coupled to the superconductor through the coupling capacitor C .

sponse corresponds to the effective conductance G_0 . The delayed response is due to the interference of the Majorana excitations created by the voltage pulse at $t = 0$. A similar effect (beyond the linear response analyzed here) was considered in Ref. [29]. The delayed response corresponds either to the normal or the Andreev reflection depending on the number of vortices in the island. In this chiral interferometer, the Andreev and normal reflections occur as a forward scattering from the incident into the outgoing Dirac channel. These are non-local in space and time processes with the amplitudes determined by the phases acquired by chiral Majorana excitations. Due to the spin texture of the Majorana modes a relative Berry phase π is acquired in addition to the relative topological phase $n\pi$ due to n vortices in the superconductor. Hence, the Andreev reflection regime is associated with odd $n = 2k + 1$ and the normal with even $n = 2k$, $k \in \mathbb{Z}$.

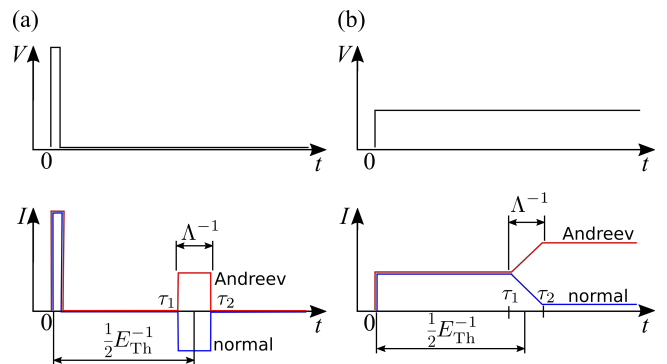


FIG. 2: Response of the current $I(t)$ to voltage pulses $V(t)$ applied to the superconducting island of the interferometer. (a) The delta-function-like pulse of $V(t)$ (upper panel) induces two response signals (lower panel): an instantaneous delta-pulse and a delayed step-pulse at $t \in [\tau_1; \tau_2]$. If the integral over the voltage pulse equals to the normal flux quantum, $V(t) = \frac{2\pi\hbar}{e}\delta(t)$, then the instantaneous peak in $I(t)$ transfers a $+e$ charge (at any temperature) and the delayed pulse $-$ a decreased charge $\pm\alpha_T e$ in the Andreev (normal) reflection regime. For a voltage pulse with an integral corresponding to the superconducting flux quantum the transferred charges are halved, as discussed in Ref. [29]. Note that voltage pulses of such weights go beyond the linear response considered here. (b) A step-like $V(t)$ (upper panel) induces an instantaneous step-like response with the conductance $G = G_0$ and a delayed response at $t \in [\tau_1; \tau_2]$. In the latter G interpolates linearly from G_0 to $G_0 \pm \alpha_T G_0$ in the Andreev (normal) reflection regime.

At zero temperature, for the step-like voltage pulse the current finally stabilizes at the value corresponding to conductance $G = 2G_0$ in the Andreev reflection regime or $G = 0$ in the normal reflection regime (see Fig. 2(b)). At finite T , the conductance saturates at the values attenuated by thermal fluctuations, $G_\pm = G_0 \pm \alpha_T G_0$, with $\alpha_T = \frac{\pi T}{\Lambda \sinh \frac{\pi T}{\Lambda}}$. At high temperatures, $T \gg \Lambda$, we obtain $G_\pm \rightarrow G_0$, which corresponds to a completely suppressed interference between the two Majorana branches.

The ac response Y_ω depends on both E_{Th} and Λ , whereas, the dc response calculated in Refs. [14, 15] does not involve E_{Th} . We note that the admittance Y_ω calculated here between points 1 and 2 assumes that the source and drain are grounded (see Fig. 1(a)). In Refs. [14, 15], the dc conductance was calculated in the alternative setting where the drain and the superconductor were grounded. The zero frequency limit for the admittance, $Y_{\omega=0}$, reproduces the results of those works for dc conductances in the linear response limit.

Proposed measurement. We propose to couple the superconducting island to a microwave waveguide (transmission line), as shown in Fig. 1(b). One should be able to measure the reflection amplitude given by

$$\lambda_\omega = -1 + \frac{2Z_{\text{TL}}}{Z_{\text{TL}} + 1/(-i\omega C) + 1/(Y_\omega - i\omega C_0)}. \quad (2)$$

Here, Z_{TL} is a transmission line impedance, which in an idealized situation approaches $Z_0 \approx 376.7\text{Ohm}$, the free space impedance. The experimentally relevant capacitances should be of the same order, $C \sim C_0$. The reflection coefficient is close to $\lambda = -1$. This means that the measured response is determined by the fine structure constant, $\alpha = Z_0 G_0 \approx \frac{1}{137}$, i.e., the effect is of the order of 1%.

The function λ_ω shows decaying oscillations as a function of ω with periods proportional to E_{Th} and Λ (see Figs. 3(a) and (b)).

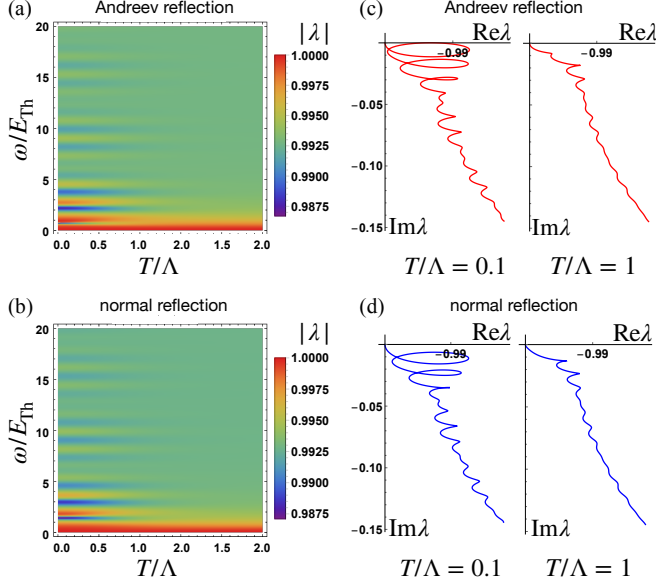


FIG. 3: Reflection coefficient $\lambda(\omega)$ as a function frequency ω and temperature T . (a) $|\lambda|$ in the Andreev reflection regime with odd n and (b) $|\lambda|$ in the normal reflection regime with even n . $|\lambda|$ oscillates as a function of ω with two sub-periods given by Λ and E_{Th} . The amplitude of oscillations decays exponentially with T . The deviation of $|\lambda|$ from unity is of order $\sim 1\%$. Data shown for asymmetric device $l_2/l_1 = 4/3$ and $\Lambda/E_{Th} = 7$. The charging energy is equal to the level spacing, which means $E_c = 2\pi E_{Th}$, or $C_0 = \frac{C_0}{v} \frac{l_1 + l_2}{2}$. We also assume $C = C_0$. (c) and (d) Parametric plots of $\text{Re}\lambda(\omega)$ and $\text{Im}\lambda(\omega)$ for $\omega \in [0, 20E_{Th}]$.

Two possible physical realizations of the interferometer are depicted in Fig. 4. The first realization is a QAHI film covered by a superconductor as shown in Fig. 4(a). The second realization is a 3D topological insulator covered with magnetic insulators of opposite magnetizations, and a superconductor (Fig. 4(b)).

A sketch of the derivation. We first describe the mean-field situation in which the superconducting order parameter Δ does not fluctuate. Since we have just a single superconducting island we can assume Δ to be real. The Bogoliubov-de Gennes equations describing setups like those in Fig. 4(b) have been extensively discussed in the literature [5, 14]. At low energies, only the Dirac or Majorana edge modes are relevant since the

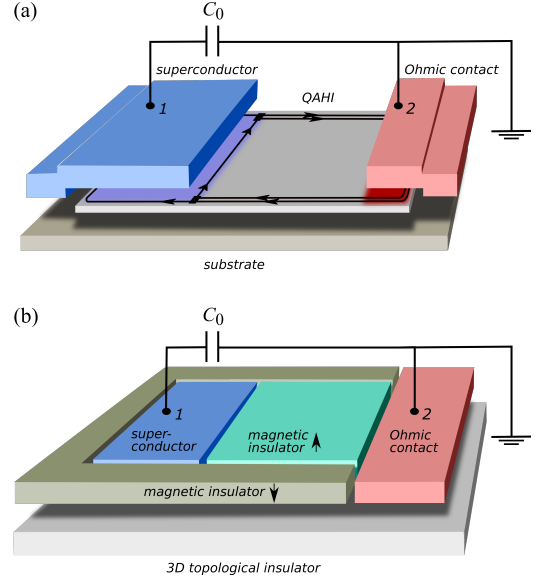


FIG. 4: Possible physical realizations of the interferometer. (a) A heterostructure composed of QAHI and a superconducting island. Incident Dirac modes (double lines) split at the Y-splittings (black bars) into Majorana modes (single lines), which surround topological superconducting region (light purple shaded region). (b) The device is realized on top of a 3D topological insulator, which is covered by magnetic insulators with opposite magnetizations (up and down arrows) and a superconductor. Chiral Dirac fermions propagate along the magnetic domain walls and convert into Majorana modes at the interface to the superconducting area.

bulk is gapped everywhere. For the Dirac edge mode, which emerges from the source, the action reads $\mathcal{S}_{in}[\psi] = \int dx_1 dt_1 dx_2 dt_2 \bar{\psi}_{in}(x_1, t_1) \mathbf{G}^{-1}(x_1, x_2, t_1, t_2) \psi_{in}(x_2, t_2)$. For the relevant values of x_1 and x_2 (between the source and the first Y-splitting) the inverse propagator \mathbf{G}^{-1} is obtained by the Fourier transform of

$$\mathbf{G}_{k,\omega}^{-1} = \begin{bmatrix} \omega - vk + i0(1-2n_k) & -2ion_k \\ 2io(1-n_k) & vk - \omega + i0(1-2n_k) \end{bmatrix}. \quad (3)$$

Here, $n_k = 1/(1 + \exp \frac{vk}{T})$ is the equilibrium distribution function dictated by the Ohmic contact, and o is an infinitesimal positive frequency. This is a matrix in the $+/-$ basis of the Keldysh space (Pauli matrices in this space are denoted by $\boldsymbol{\sigma}$) [30]. Introducing the Nambu spinor $\check{\Psi}_{in} = [\psi_{in}, \bar{\psi}_{in}]^T$ we rewrite the action as $\mathcal{S}_{in}[\check{\Psi}_{in}] = \frac{1}{2} \int \check{\Psi}_{in} \check{\tau}_x \check{\mathbf{G}}^{-1} \check{\Psi}_{in}$, where $\check{\mathbf{G}}_{k,\omega}^{-1} = \check{\tau}_+ \check{\tau}_- \mathbf{G}_{k,\omega}^{-1} + \check{\tau}_- \check{\tau}_+ [\mathbf{G}_{-k,-\omega}^{-1}]^T$ and $\check{\tau}_\pm = \frac{1}{2}(\check{\tau}_x \pm i\check{\tau}_y)$. The Pauli matrices $\check{\tau}$ act in the Gor'kov-Nambu particle-hole space and $\tau_z = \pm 1$ correspond to electron-like or hole-like state in the Dirac channel.

The scattering matrix \check{R} for the lower (first) Y-splitting describes the conversion of an incident Dirac electron and

hole into a pair of Majorana particles χ_k and η_k :

$$\begin{bmatrix} \chi_{\text{out};k} \\ \eta_{\text{out};k} \end{bmatrix} = \check{R} \begin{bmatrix} \psi_{\text{in};k} \\ \bar{\psi}_{\text{in};-k} \end{bmatrix}, \quad \check{R} = \begin{bmatrix} \frac{1}{\sqrt{2}} & \frac{1}{\sqrt{2}} \\ \frac{i}{\sqrt{2}} & \frac{-i}{\sqrt{2}} \end{bmatrix}. \quad (4)$$

The Hermitian conjugated \check{R}^+ of the upper (second) Y-splitting describes the conversion of Majorana modes into outgoing Dirac fermions: $\begin{bmatrix} \psi_{\text{out};k} \\ \bar{\psi}_{\text{out};-k} \end{bmatrix} = \check{R}^+ \begin{bmatrix} \chi_{\text{in};k} \\ \eta_{\text{in};k} \end{bmatrix}$. Finally, a relation between in- and out- Dirac states $\check{\Psi}_{\text{in};k} = [\psi_{\text{in};k} \ \bar{\psi}_{\text{in};-k}]^T$ and $\check{\Psi}_{\text{out};k} = [\psi_{\text{out};k} \ \bar{\psi}_{\text{out};-k}]^T$ reads

$$\check{\Psi}_{\text{out};k} = \check{S}_k \check{\Psi}_{\text{in};k}. \quad (5)$$

Here, the scattering matrix is found as $\check{S}_k = \check{R}^+ \check{F}_k \check{R}$ where $\check{F}_k = \text{diag}\{(-1)^{n+1} e^{ikl_1}, e^{ikl_2}\}$ determines Berry and topological phases, and dynamic phases $kl_{1,2}$ of coherently propagating Majorana excitations.

With the help of the above introduced scattering matrix we now transform from the basis of incoming Dirac states to the basis of exact scattering states. That is, the field $\check{\Psi}_k$ now annihilates an exact scattering state in the whole setup. The action retains its form, i.e., $\mathcal{S}_0[\check{\Psi}] = \frac{1}{2} \int \check{\Psi} \check{\tau}_x \check{\mathbf{G}}^{-1} \check{\Psi}$.

The scattering matrix allows us to represent the current flowing into the island, $I = ev(\bar{\psi}_{\text{in}}\psi_{\text{in}} - \bar{\psi}_{\text{out}}\psi_{\text{out}})$, as

$$I[\Psi] = \frac{1}{2} \Psi_p \check{\tau}_x \check{J}_{p,k} \Psi_k, \quad (6)$$

where the matrix $\check{J}_{p,k} = v\check{\tau}_z - v\check{S}_p^+ \check{\tau}_z \check{S}_k$ has a non-diagonal structure in momentum and Gor'kov-Nambu spaces.

Next we allow the phase Φ of the order parameter $\Delta = |\Delta|e^{i\Phi}$ to fluctuate. We perform a standard gauge transformation of fermion phases [30–32], which makes the superconducting order parameter real, $|\Delta|e^{i\Phi} \rightarrow |\Delta|$. The Majorana edge modes are transformed accordingly and we extend the gauge transformation infinitesimally into the incoming and outgoing Dirac modes. That is $\psi_{\text{in}}(x, t) \rightarrow \exp[\frac{i}{2}\theta(x - (z_1 - \epsilon))\Phi(t)]\psi_{\text{in}}(x, t)$, where z_1 is the coordinate of the first Y-splittings and $\epsilon \rightarrow 0$ at the later stage of the derivation. Similarly $\psi_{\text{out}}(x, t) \rightarrow \exp[\frac{i}{2}\theta((z_2 + \epsilon) - x)\Phi(t)]\psi_{\text{out}}(x, t)$, where z_2 is the coordinate of the second Y-splitting. The discrete symmetry $\Phi \rightarrow \Phi + 4\pi$ is preserved.

In the above discussed gauge transform, we encounter the theta-function regularization problem because we go beyond the long wave-length approximation. We resolve it using a discretized tight-binding approach [34]. As a result, we obtain an interaction term in the action $\mathcal{S}_{\text{int}} = \int dt (\frac{1}{e} \sin \Phi/2 + \frac{U}{\hbar} (\cos \Phi/2 - 1))$. This is an alternative to inserting [30–32] the phase variable into the scattering matrices of the system [35]. Here $U = \hbar av(\bar{\psi}_{\text{in}}\psi'_{\text{in}} + \bar{\psi}_{\text{out}}\psi'_{\text{out}})$ with a being the lattice constant. It is important to keep here the term $\propto U$,

although one could be tempted to drop it in the continuous long wave-length limit. This term provides an important regularization in what follows.

These steps lead to the following effective action on the Keldysh contour \mathcal{C}

$$\mathcal{S}[\Psi, \Phi] = \int_{\mathcal{C}} \left[\frac{\hbar \dot{\Phi}^2}{16E_c} + \frac{1}{2e} \Phi I[\Psi] - \frac{\omega_c}{8\pi^2} \Phi^2 \right] dt + \mathcal{S}_0[\Psi]. \quad (7)$$

(We set $e = \hbar = k_B = 1$ below and restore them in final expressions.) The first term in (7) is the usual charging energy, where we have employed the Josephson relation $V = \Phi/2$, V being the scalar potential. We assume that the fluctuations of phase Φ are small (quasi-classical regime) because of large C_0 . Thus we have expanded \mathcal{S}_{int} up to a quadratic order in Φ . This yields the second term giving a linear coupling of the phase variable to the current fluctuations, and the third one, which plays a role of the diamagnetic counter term. It involves a divergent negative energy of the ground state $\langle U \rangle = -av\frac{k_c^2}{2\pi}$. The cutoff momentum is chosen as $k_c = \frac{2}{\pi a}$ such that the upper frequency cutoff in our theory, $\omega_c = vk_c$, and we obtain $\langle U \rangle = \omega_c/\pi^2$.

Integrating over Ψ we obtain the effective action for the phase $\mathcal{S}[\Phi] = -i \ln[\int D[\Psi] \exp(i\mathcal{S}[\Psi, \Phi])]$. It reads

$$\begin{aligned} \mathcal{S}[\Phi] = & \int \Phi_q(t) \left(\frac{\omega_c}{16\pi^2} - \frac{1}{8E_c} \partial_t^2 \right) \Phi_{\text{cl}}(t) dt - \\ & - i \frac{1}{2} \text{Tr} \ln \left[\check{1} + \check{\mathbf{G}}_p(t-t') \check{J}_{p,k} (\boldsymbol{\sigma}_x \Phi_{\text{cl}}(t') + \boldsymbol{\sigma}_0 \Phi_q(t')) \right]. \quad (8) \end{aligned}$$

(The prefactor 1/2 in front of $\text{Tr} \ln$ is due the Pfaffian, which appears after the integration over the non-independent Grassmann fields in the Gor'kov-Nambu formalism.) The Keldysh rotation from $\Phi(t_{\pm})$ to the classical and quantum components, $\Phi_{\text{cl}}(t) = \frac{1}{2}(\Phi(t_+) + \Phi(t_-))$ and $\Phi_q(t) = \Phi(t_+) - \Phi(t_-)$, is performed. In the quasi-classical approach we expand (8) up to second order in Φ_{cl} and Φ_q . This gives a dissipative action of the Caldeira-Leggett type [33]:

$$\begin{aligned} \mathcal{S}[\Phi] = & \frac{1}{8} \int \frac{\omega^2}{E_c} \Phi_{q,-\omega} \Phi_{\text{cl},\omega} \frac{d\omega}{2\pi} + \frac{1}{8} \int \frac{d\omega}{2\pi} \times \\ & \begin{bmatrix} \Phi_{\text{cl},-\omega} & \Phi_{q,-\omega} \end{bmatrix} \begin{bmatrix} 0 & -i\omega Y_{\omega}^* \\ i\omega Y_{\omega} & i\text{Re}[Y_{\omega}] \omega \coth \frac{\omega}{2T} \end{bmatrix} \begin{bmatrix} \Phi_{\text{cl},\omega} \\ \Phi_{q,\omega} \end{bmatrix}. \quad (9) \end{aligned}$$

This action is represented in Keldysh $\boldsymbol{\sigma}$ -space where the matrix possesses the causality structure [30]. There are retarded and advanced parts of the current correlator in the off-diagonal of this matrix. The Keldysh term in the right bottom corner reproduces fluctuation-dissipation theorem in this methodology. We note that the second order expansion of the logarithm produces a divergent term, which, as usual, appears in Caldeira-Leggett theory

with linearized coupling between Φ and I . The diamagnetic counter-term in (7) ($\propto \omega_c$) cancels this divergence.

Conclusions. We have analyzed the microwave dynamics of a Majorana interferometer with floating superconducting island in the linear response regime. We show that one can observe the propagation and interference of Majorana excitations in the two branches of the interferometer by measuring the spectrum of microwaves reflected by the system. This is an alternative to proposals dealing with the detection of current and noise in the Ohmic contacts (sources or drains) of the interferometers. The proposed technique could also be used in the time-resolved manner, i.e., by sending microwave pulses and observing the response delayed due to the finite propagation time and the interference of the Majorana excitations.

Acknowledgements. We thank I. Pop for insightful discussions. This research was financially supported by the DFG-RFBR Grant [No. MI 658/12-1, SH 81/6-1 (DFG) and No. 20-52-12034 (RFBR)].

* Electronic address: shapiro.dima@gmail.com

- [1] X.-L. Qi and S.-C. Zhang, *Rev. Mod. Phys.* **83**, 1057 (2011).
- [2] J. Alicea, Reports on progress in physics **75**, 076501 (2012).
- [3] C. Beenakker, *Annual Review of Condensed Matter Physics* **4**, 113 (2013).
- [4] C. Kallin and J. Berlinsky, *Reports on Progress in Physics* **79**, 054502 (2016).
- [5] L. Fu and C. L. Kane, *Phys. Rev. Lett.* **100**, 096407 (2008).
- [6] Q. L. He, L. Pan, A. L. Stern, E. C. Burks, X. Che, G. Yin, J. Wang, B. Lian, Q. Zhou, E. S. Choi, K. Murata, X. Kou, Z. Chen, T. Nie, Q. Shao, Y. Fan, S.-C. Zhang, K. Liu, J. Xia, and K. L. Wang, *Science* **357**, 294 (2017).
- [7] J. Shen, J. Lyu, J. Z. Gao, Y.-M. Xie, C.-Z. Chen, C.-w. Cho, O. Atanov, Z. Chen, K. Liu, Y. J. Hu, K. Y. Yip, S. K. Goh, Q. L. He, L. Pan, K. L. Wang, K. T. Law, and R. Lortz, *Proceedings of the National Academy of Sciences* **117**, 238 (2020).
- [8] M. Kayyalha, D. Xiao, R. Zhang, J. Shin, J. Jiang, F. Wang, Y.-F. Zhao, R. Xiao, L. Zhang, K. M. Fijalkowski, P. Mandal, M. Winnerlein, C. Gould, Q. Li, L. W. Molenkamp, M. H. W. Chan, N. Samarth, and C.-Z. Chang, *Science* **367**, 64 (2020).
- [9] G. C. Ménard, S. Guissart, C. Brun, R. T. Leriche, M. Trif, F. Debontridder, D. Demaille, D. Roditchev, P. Simon, and T. Cren, *Nature communications* **8**, 2040 (2017).
- [10] S. Kezilebieke, M. N. Huda, V. Vaño, M. Aapro, S. C. Ganguli, O. J. Silveira, S. Głodzik, A. S. Foster, T. Ojanen, and P. Liljeroth, *Nature* **588**, 424 (2020).
- [11] J. Li, T. Neupert, Z. Wang, A. MacDonald, A. Yazdani, and B. A. Bernevig, *Nature communications* **7**, 1 (2016).
- [12] Z. Wang, J. O. Rodriguez, L. Jiao, S. Howard, M. Graham, G. D. Gu, T. L. Hughes, D. K. Morr, and V. Madhavan, *Science* **367**, 104 (2020).
- [13] Y. Kasahara, T. Ohnishi, Y. Mizukami, O. Tanaka, S. Ma, K. Sugii, N. Kurita, H. Tanaka, J. Nasu, Y. Motome, T. Shibauchi, and Y. Matsuda, *Nature* **559**, 227 (2018).
- [14] L. Fu and C. L. Kane, *Phys. Rev. Lett.* **102**, 216403 (2009).
- [15] A. R. Akhmerov, J. Nilsson, and C. W. J. Beenakker, *Phys. Rev. Lett.* **102**, 216404 (2009).
- [16] G. Strübi, W. Belzig, T. L. Schmidt, and C. Bruder, *Physica E: Low-dimensional Systems and Nanostructures* **74**, 489 (2015).
- [17] G. Strübi, W. Belzig, M.-S. Choi, and C. Bruder, *Phys. Rev. Lett.* **107**, 136403 (2011).
- [18] J. Li, G. Fleury, and M. Büttiker, *Phys. Rev. B* **85**, 125440 (2012).
- [19] D. S. Shapiro, A. Shnirman, and A. D. Mirlin, *Phys. Rev. B* **93**, 155411 (2016).
- [20] D. S. Shapiro, D. E. Feldman, A. D. Mirlin, and A. Shnirman, *Phys. Rev. B* **95**, 195425 (2017).
- [21] D. S. Shapiro, A. D. Mirlin, and A. Shnirman, *Phys. Rev. B* **98**, 245405 (2018).
- [22] S. B. Chung, X.-L. Qi, J. Maciejko, and S.-C. Zhang, *Phys. Rev. B* **83**, 100512 (2011).
- [23] C.-X. Liu and B. Trauzettel, *Phys. Rev. B* **83**, 220510 (2011).
- [24] C.-Y. Hou, K. Shtengel, and G. Refael, *Phys. Rev. B* **88**, 075304 (2013).
- [25] B. Lian, X.-Q. Sun, A. Vaezi, X.-L. Qi, and S.-C. Zhang, *Proceedings of the National Academy of Sciences* **115**, 10938 (2018).
- [26] C. W. J. Beenakker, P. Baireuther, Y. Herasymenko, I. Adagideli, L. Wang, and A. R. Akhmerov, *Phys. Rev. Lett.* **122**, 146803 (2019).
- [27] F. Hassler, A. Grabsch, M. J. Pacholski, D. O. Oriekhov, O. Ovdad, I. Adagideli, and C. W. J. Beenakker, *Phys. Rev. B* **102**, 045431 (2020).
- [28] C. Beenakker and D. Oriekhov, *SciPost Physics* **9**, 080 (2020).
- [29] I. Adagideli, F. Hassler, A. Grabsch, M. Pacholski, and C. Beenakker, *SciPost Phys.* **8**, 13 (2020).
- [30] A. Kamenev, *Field Theory of Non-Equilibrium Systems* (Cambridge University Press, Cambridge, UK, 2011).
- [31] L. S. Levitov, H. Lee, and G. B. Lesovik, *Journal of Mathematical Physics* **37**, 4845 (1996).
- [32] A. Andreev and A. Kamenev, *Phys. Rev. Lett.* **85**, 1294 (2000).
- [33] A. O. Caldeira and A. J. Leggett, *Phys. Rev. Lett.* **46**, 211 (1981).
- [34] See Sec. A in Supplementary Material for details.
- [35] See Sec. B in Supplementary Material for details.

SUPPLEMENTARY MATERIAL

A. Derivation of the interaction part \mathcal{S}_{int} in the effective action

The derivation is based on four steps (i-iv) schematically illustrated in Fig. S1. Let us map chiral Dirac modes ψ_{in} and ψ_{out} onto a line with the coordinate x (Fig. S1 (i)). The Y-splittings are located at $x = z_{1,2}$, the incident mode ψ_{in} scatters into a pair of Majorana modes surrounding the topological superconductor with floating phase of the order parameter, $|\Delta|e^{i\Phi}$, which in turn fuse into ψ_{out} .

In the second step (see Fig. S1 (ii)), we gauge out the superconducting phase, $|\Delta|e^{i\Phi} \rightarrow |\Delta|$. We extend the gauge transformation slightly beyond the superconductor, i.e., we perform it in the interval $z_1 - \epsilon < x < z_2 + \epsilon$. For the Dirac modes the step-like gauge transformation shown in Fig. S1 (ii) reads thus as follows

$$\psi_{\text{in}}(x, t) \rightarrow e^{i\theta(x-(z_1-\epsilon))\Phi(t)/2}\psi_{\text{in}}(x, t) \quad (\text{S1})$$

and

$$\psi_{\text{out}}(x, t) \rightarrow e^{i\theta(z_2+\epsilon-x)\Phi(t)/2}\psi_{\text{out}}(x, t). \quad (\text{S2})$$

This gives two phase drops at $x = z_1 - \epsilon$ and $x = z_2 + \epsilon$, which are marked by red crosses.

In the third step we transform the chiral modes ψ_{in} and ψ_{out} to a non-chiral mode $\psi(x)$ on a semi-axis (Fig. S1 (iii)). Both phase drops are now merged into one, which is marked by the red bar. In the final step, the non-chiral ψ near the phase drop is mapped onto a 1D tight-binding lattice of fermions (Fig. S1 (iv)). The corresponding tight-binding Hamiltonian for $\Phi = 0$ reads

$$\hat{H} = \frac{it}{2} \sum_n (\hat{c}_{n+1}^\dagger \hat{c}_n - \hat{c}_n^\dagger \hat{c}_{n+1}). \quad (\text{S3})$$

It has a spectrum $\varepsilon = t \sin ka$ with $k \in [-\frac{\pi}{a}, \frac{\pi}{a}]$, t is a hopping energy and a is a lattice constant. In the low energy limit, $\varepsilon \ll t$, we obtain right (left) moving fermions near $k = 0$ ($k = \pm\frac{\pi}{a}$). These states determine the long wave-length behavior of in- and out- chiral fermions in our setting.

Now we consider two sites, $n = m$ and $n = m + 1$, where the phase drop $\Phi \neq 0$ occurs (it is shown by the red cross in Fig. S1 (iv)). The discrete version of the gauge transform (S1, S2) corresponds to $\pm\Phi/2$ phase shifts accumulated when a fermion hops between these sites. The modification of the matrix elements describing the hopping between sites m and $m + 1$, $t \rightarrow te^{\pm i\Phi/2}$, in (S3) results in $\delta\hat{H}$ being added to the full Hamiltonian, $\hat{H} \rightarrow \hat{H} + \delta\hat{H}$. Here

$$\delta\hat{H} = \frac{it}{2} \int \frac{dkdp}{(2\pi)^2} \hat{c}_k^\dagger \hat{c}_p [e^{-ipa}(e^{i\frac{\Phi}{2}} - 1) - e^{-ika}(e^{-i\frac{\Phi}{2}} - 1)]. \quad (\text{S4})$$

(Without loss of generality we set $m = -1$ in this expression.) The low energy limit of $\delta\hat{H}$ yields \mathcal{S}_{int} after identifying $ta \rightarrow v$, $\hat{c}_k \rightarrow \psi_{\text{in}}$ at $ka \ll 1$, and $\hat{c}_k \rightarrow \psi_{\text{out}}$ at $ka \approx \pm\pi$. After the transition to this long wavelength limit we send ϵ to zero.

B. Non-stationary scattering matrix

Alternatively to the use of the step-like gauge transform that extends infinitesimally into the incoming and the outgoing Dirac modes and that results in \mathcal{S}_{int} , one can embed the superconducting phase into a non-stationary scattering matrix $S_\Phi(t, t')$, similarly to [30–32]. This scattering matrix incorporates the propagation in the Majorana

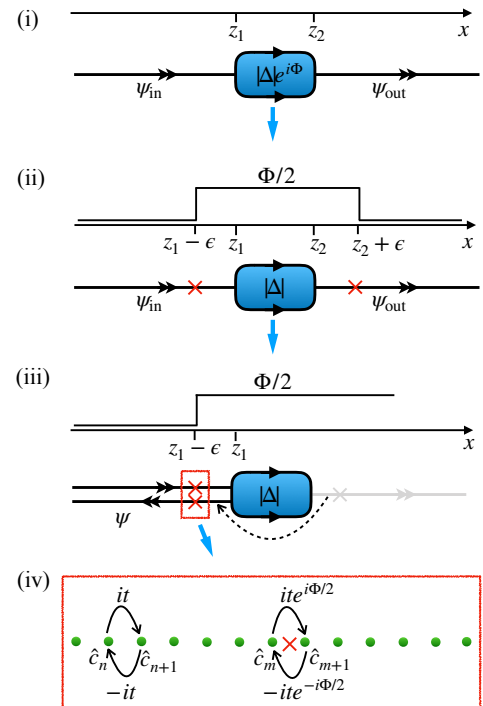


FIG. S1: Schematic derivation of \mathcal{S}_{int} : (i) representation of chiral modes on a line, (ii) gauge transformation (S1, S2), (iii) mapping onto non-chiral mode, and (iv) mapping of the mode ψ near the phase drop onto a fermion lattice with $\hat{H} + \delta\hat{H}$.

edge channels and relates the local Dirac fields near the respective Y-splittings, $\check{\Psi}_{\text{out}}(z_2 + \epsilon, t) = \int \check{S}(t, t') \check{\Psi}_{\text{in}}(z_1 - \epsilon, t') dt'$. Here, $\check{S}(t - t') = \check{R}^+ \check{F}(t - t') \check{R}$ and $\check{F}(t) = v \int \frac{dk}{2\pi} \check{F}_k e^{-ivkt} = \text{diag}\{(-1)^{n+1} \delta(t - \tau_1), \delta(t - \tau_2)\}$. After the gauge transformation the scattering matrix acquires the form

$$\check{S}_{\Phi}(t, t') = e^{-\frac{i}{2} \check{\tau}_z (\sigma_0 \Phi_c(t) + \sigma_z \Phi_q(t)/2)} \check{S}(t - t') e^{\frac{i}{2} \check{\tau}_z (\sigma_0 \Phi_c(t') + \sigma_z \Phi_q(t')/2)}, \quad \{t, t'\} \in [-\infty, \infty]. \quad (\text{S5})$$

Integrating now over the fermionic degrees of freedom in the spirit of Refs. [30, 32] one could obtain the effective action for the phase variable Φ .